TEMPERATURE INDUCED BANDGAP TUNING AND STRUCTURAL EVOLUTION IN ELECTROCHEMICALLY DEPOSITED NANOCRYSTALLINE MgS THIN FILMS

Ernest O. Ojegu[1], Erhieyovwe Akpata[1], Blessing Odia Ogo[2], Imosobomeh L. Ikhioya[3*]

[1]*Department of Physics, Delta State University, Abraka, Delta State, Nigeria*
[2]*Delta State College of Education, Mosogar, Delta State, Nigeria*
[3]*Department of Physics, Federal University Lokoja, Kogi State, Nigeria*

**Corresponding author: imosobomeh.ikhioya@fulokoja.edu.ng*

Cite this article as: *Ojegu, E.O., Akpata, E., Ogo, B.O. and Ikhioya, I.L. (2026). Temperature induced bandgap tuning and structural evolution in electrochemically deposited nanocrystalline MgS thin films. Journal of Interdisciplinary Postgraduate Research, 2(1), 288–299.*

Abstract

This study presents the synthesis and characterization of nanocrystalline magnesium sulfide (MgS) thin films prepared via the electrochemical deposition technique at varying precursor temperatures. Structural analysis using X ray diffraction (XRD) confirms the polycrystalline nature of all deposited samples, with four distinct diffraction peaks indexed to the (011), (111), (200), and (211) planes. Although bulk MgS typically adopts a cubic rock salt structure, the observed indexing suggests possible variations in symmetry or phase composition influenced by the deposition conditions. Electrical characterization reveals a direct proportionality between resistivity and both temperature and film thickness, with resistivity values increasing from 74.97×10^7 Ω·cm to 79.88×10^7 Ω·cm as the deposition temperature was raised from room temperature to 45 °C. This trend is attributed to changes in grain size and structural defects that impede charge carrier mobility in thicker films. Optical analysis shows high transparency in the visible spectrum (400 to 700 nm), with absorbance values remaining low (0.1 to 0.4 a.u.). Notably, increasing the deposition temperature from room temperature to 45 °C resulted in a significant optical bandgap shift from 1.50 eV to 2.38 eV. These findings indicate that higher temperature MgS films are excellent candidates for UV photodetectors and window layers in photovoltaic cells due to their expanded transparency range.

Keywords: *Electrochemical deposition; Magnesium sulfide; Optical analysis; X ray diffraction; Cubic rock salt structure; Band gap tuning; Thin films; Nanocrystalline*

1. Introduction

Magnesium sulfide (MgS) is a II–VI wide bandgap semiconductor that has attracted growing research interest owing to its favourable combination of optical transparency, chemical stability, and structural versatility. The material crystallises predominantly in the cubic rock salt (NaCl type) structure under equilibrium conditions, although hexagonal wurtzite and zinc blende polymorphs have also been reported under certain synthesis conditions (Drief *et al.*, 2004). With a bulk band gap of approximately 2.42 eV, MgS occupies a strategic position in the family of alkaline earth chalcogenides, offering potential for applications spanning light emitting diodes, flame retardant materials, ultraviolet photodetectors, and window layers in thin film solar cells (Agrawal *et al.*, 2022).

The luminescence properties of MgS are of particular significance. The short metal to sulfur bond distance in the rock salt lattice facilitates efficient radiative recombination pathways, rendering the material attractive for solid state lighting applications (Sharif *et al.*, 2019). Furthermore, quantum confinement effects emerge when MgS is prepared in nanocrystalline form, enabling the electronic and optical properties to be tailored through careful control of grain size and morphology (Geetha *et al.*, 2017). The lattice compatibility of MgS with many commercially important semiconductors adds to its appeal as a heterostructure component in multilayer photovoltaic and optoelectronic device architectures (Bradford, 2003).

Thin film technology plays a central role in realising the size dependent properties of semiconductors for practical device integration. By confining the active material to thicknesses ranging from a few nanometres to several hundred nanometres, high performance surfaces can be fabricated with minimal consumption of raw material, thereby reducing both cost and environmental impact (Samuel *et al.*, 2023a). Metal sulfide thin films are especially promising for photovoltaic applications because their wide band gaps enable the capture of a substantial portion of the solar spectrum while maintaining high visible transparency (Muthuraj, 2021). The choice of deposition technique profoundly influences the crystallographic, morphological, and optical characteristics of the resulting films.

Several methods have been employed for the preparation of MgS thin films and related nanostructures, including chemical bath deposition (Geetha *et al.*, 2017), thermal evaporation, and sol gel processing. Among these, the electrochemical deposition (ECD) method stands out for its simplicity, low cost, and precise control over film thickness and composition through regulation of the applied potential, current density, and bath temperature (Ijeh *et al.*, 2024; Samuel *et al.*, 2023b). In ECD, controlled redox reactions take place within a three electrode cell containing an electrolytic bath, and the reference electrode (Ag/AgCl) provides the stable ground voltage necessary for accurate monitoring of the working electrode potential (Ikhioya and Nkele, 2024; Ikhioya *et al.*, 2023a).

Despite the acknowledged potential of MgS in optoelectronics, only limited studies have systematically examined how deposition temperature affects the structural, electrical, and optical properties of electrochemically deposited MgS thin films. Temperature is a critical synthesis parameter because it governs the kinetics of ionic transport, nucleation density, and grain growth at the substrate interface (Okechukwu *et al.*, 2024). The present study addresses this gap by reporting the synthesis and comprehensive characterization of nanocrystalline MgS thin films deposited at four distinct precursor temperatures, namely room temperature, 35 °C, 40 °C, and 45 °C. The structural evolution, electrical transport behaviour, and optical properties of the films are examined in detail, with particular emphasis on the temperature induced tuning of the optical band gap.

2. Experimental Details

2.1 Materials and Precursor Preparation

The precursor chemicals employed in this study were magnesium nitrate hexahydrate ($Mg(NO_3)_2 \cdot 6H_2O$) and sodium sulfate (Na_2SO_4), both of analytical grade purity. A 0.1 mol solution of each salt was prepared by dissolving the appropriate mass in deionised water under continuous magnetic stirring until homogeneous solutions were obtained. Fluorine doped tin oxide (FTO) coated glass substrates (2.5 cm × 1.5 cm) served as the working electrode. Prior to deposition, the substrates were cleaned sequentially with detergent, rinsed in deionised water, and dried to remove surface contaminants.

2.2 Electrochemical Deposition

The deposition was carried out in a three electrode electrochemical cell comprising the FTO substrate as the cathode, a platinum counter electrode as the anode, and a silver/silver chloride (Ag/AgCl) reference electrode. Equal volumes of the magnesium and sulfate precursors were combined in the electrolytic bath. A potentiostatic condition of –200 mV versus the standard calomel electrode (SCE) was maintained for 5 seconds during each deposition cycle. Four sets of films were prepared by varying the precursor bath temperature from room temperature (approximately 28 °C) to 35 °C, 40 °C, and 45 °C. After deposition, the films were dried using a hand dryer and subsequently annealed at moderate temperature for 20 minutes to relieve internal stress. The deposited films were then characterised using X ray diffraction

(XRD), UV Vis spectrophotometry, and electrical resistivity measurements (Ikhioya and Nkele, 2023a; Ikhioya and Nkele, 2023b).

3. Results and Discussion

3.1 Structural Analysis

The X ray diffraction patterns of the MgS thin films deposited at room temperature, 35 °C, 40 °C, and 45 °C are presented in Figure 1. All four samples exhibit well defined diffraction peaks at specific scattering angles (2θ), which are indexed with Miller indices (hkl) corresponding to the (011), (111), (200), and (211) crystallographic planes. The presence of sharp, clearly resolved peaks across all deposition temperatures confirms the polycrystalline nature of the synthesised films. A preferred orientation along the (111) plane is evident in all samples, as indicated by the consistently higher intensity of this reflection relative to the other observed peaks.

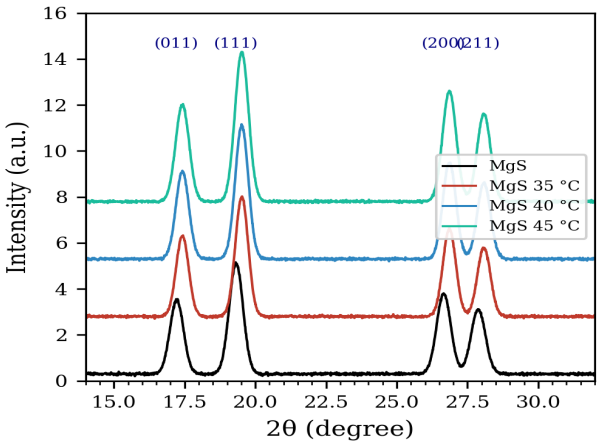

Figure 1: *X ray diffraction patterns of MgS nanostructured thin films deposited at room temperature, 35 °C, 40 °C, and 45 °C.*

Although bulk MgS crystallises in the cubic rock salt structure, the simultaneous observation of (011) and (211) peaks alongside the (111) and (200) reflections warrants careful interpretation. The coexistence of these indices may indicate subtle variations in crystal symmetry or the presence of a secondary phase that develops under specific deposition conditions. Similar deviations from the ideal rock salt diffraction pattern have been reported for nanocrystalline alkaline earth chalcogenides prepared by solution based methods (Drief *et al.*, 2004; Geetha *et al.*, 2017). It is plausible that the low temperature electrochemical synthesis route favours the stabilisation of metastable phases that are not thermodynamically accessible under equilibrium growth conditions.

A clear trend is observed in the evolution of peak intensity with deposition temperature. The (111) and (200) peaks increase in intensity as the temperature rises from room temperature to 45 °C, indicating an improvement in the degree of crystallinity or an increase in the volume fraction of the crystalline phase. The sharpening of the diffraction peaks at elevated temperatures, as quantified by the full width at half maximum (FWHM), further supports the conclusion that higher deposition temperatures promote the formation of larger, more ordered crystallites (Akpu *et al.*, 2023a). Notably, the peak positions (2θ values) remain stable across all temperatures, confirming that the lattice parameters and unit cell dimensions of the MgS phase are insensitive to the modest temperature variations employed in this study.

Table 1. Structural parameters of MgS nanostructured thin films deposited at varying temperatures.

Film	2θ (°)	d (Å)	Å	β	(hkl)	D (nm)	σ (×10¹■)
MgS	17.22	5.147	8.915	0.564	011	0.248	4.919
	19.32	4.592	9.185	0.578	111	0.243	5.136
	26.66	3.342	6.685	0.589	200	0.242	5.196
	27.88	3.199	7.155	0.599	211	0.238	5.346
MgS 35°C	17.42	5.089	8.815	0.524	011	0.267	4.244
	19.56	4.537	9.074	0.537	111	0.262	4.430
	26.79	3.327	6.654	0.539	200	0.264	4.349
	27.99	3.187	7.126	0.541	211	0.264	4.359
MgS 40°C	17.42	5.089	8.815	0.544	011	0.258	4.574
	19.56	4.537	9.074	0.547	111	0.257	4.596
	26.79	3.327	6.654	0.549	200	0.259	4.512
	27.99	3.187	7.126	0.552	211	0.259	4.538
MgS 45°C	17.42	5.089	8.815	0.564	011	0.248	4.916
	19.56	4.537	9.074	0.567	111	0.248	4.939
	26.79	3.327	6.654	0.569	200	0.250	4.847
	27.99	3.187	7.126	0.563	211	0.254	4.721

The structural parameters extracted from the XRD data using Equations (1) to (3) are summarised in Table 1. The Scherrer equation (Equation 1) was used to estimate the crystallite size (D) from the peak broadening, the interplanar spacing (d) was obtained from the Bragg condition (Equation 2), and the dislocation density (σ) was calculated from the inverse square of the crystallite size (Equation 3). An inverse proportionality between the FWHM and the crystallite size is clearly observed: as the FWHM increases, the crystallite size decreases, consistent with the Scherrer formalism. The films deposited at 35 °C exhibit the largest average crystallite size (0.264 nm), suggesting that this temperature optimises the balance between nucleation rate and grain growth kinetics during the electrochemical

deposition process (Akpu, 2023b; Ikhioya and Nkele, 2023b).

$$D = k\lambda / \beta \cos\theta \quad (1)$$

$$d = \lambda / 2 \sin\theta \quad (2)$$

$$\sigma = 1 / D^2 \quad (3)$$

where k = 0.94 is the Scherrer constant, λ = 0.154 nm is the wavelength of the Cu Kα X ray source, θ is the Bragg diffraction angle, and β is the FWHM of the diffraction peak in radians. Figure 8 presents the variation of average crystallite size and dislocation density with deposition temperature. The dislocation density, which quantifies the concentration of lattice imperfections per unit area, decreases as the crystallite size increases, confirming the inverse square relationship embedded in Equation (3). Films deposited at 35 °C display the lowest dislocation density, implying a more ordered crystalline lattice with fewer structural defects (Ali *et al.*, 2023; Ikhioya and Nkele, 2023c).

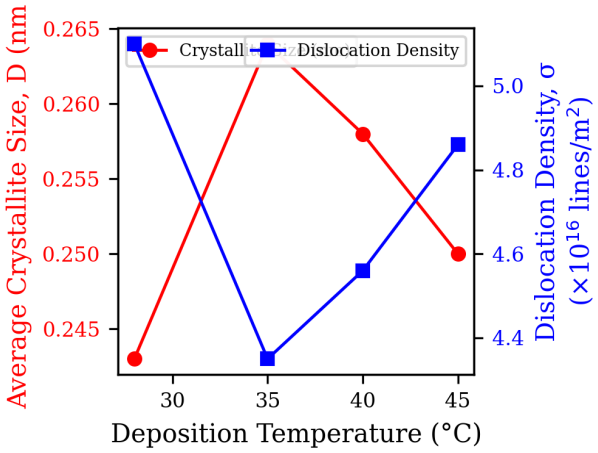

Figure 8: *Variation of average crystallite size and dislocation density with deposition temperature for MgS thin films.*

3.2 Electrical Properties

The electrical properties of the MgS thin films are summarised in Table 2 and illustrated in Figure 2. As the deposition temperature increases from room temperature to 45 °C, the film thickness increases steadily from 107.55 nm to 110.97 nm. This observation suggests that higher thermal energy during deposition enhances the rate of ionic transport and surface reaction kinetics at the substrate, leading to the accumulation of a thicker deposited layer (Onye buchi, 2026; Sarwar *et al.*, 2023).

Table 2. Electrical properties of MgS nanostructured thin films.

Sample	t (nm)	ρ (Ω·cm) ×10■	σ (S/m) ×10■■
MgS (RT)	107.55	74.97	1.33
MgS 35 °C	109.12	78.54	1.27
MgS 40 °C	110.23	79.21	1.26
MgS 45 °C	110.97	79.88	1.25

The electrical resistivity exhibits a direct proportional relationship with both temperature and film thickness, increasing from 74.97 × 10^7 Ω·cm at room temperature to 79.88 × 10^7 Ω·cm at 45 °C. In semiconductor physics, an increase in resistivity with film thickness is frequently attributed to changes in grain boundary density and an accumulation of structural defects that impede the flow of charge carriers (Samuel *et al.*, 2023a; Saba *et al.*, 2025). The corresponding electrical conductivity, which is the mathematical reciprocal of resistivity (σ = 1/ρ), decreases from 1.33 × 10^{-6} S/m to 1.25 × 10^{-6} S/m over the same temperature range.

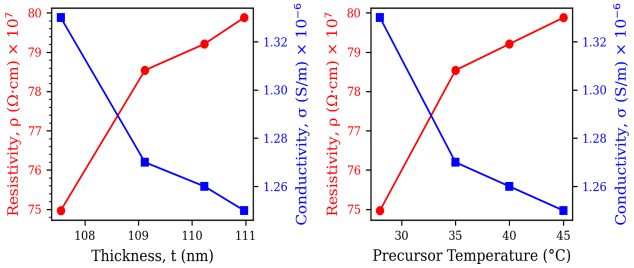

Figure 2: *Variation of resistivity and conductivity with film thickness (left) and precursor temperature (right) for MgS thin films.*

The very low conductivity values (in the 10^{-6} S/m range) confirm that the MgS thin films behave as wide bandgap semiconductors or near insulators under the present deposition conditions. The incremental and linear nature of the changes across the temperature series, without sudden discontinuities, indicates a stable and controlled deposition process (Ikhioya *et al.*, 2023b). The high resistivity values further suggest that the films may be near stoichiometric with low intrinsic carrier concentrations at these deposition temperatures. The progressive increase in resistivity with temperature is attributable to enhanced electron scattering at grain boundaries as the film becomes thicker and potentially denser (Okechukwu *et al.*, 2024).

3.3 Optical Absorbance

The optical absorbance spectra of the MgS thin films deposited at room temperature, 35 °C, 40 °C, and 45 °C are presented in Figure 3. All four samples exhibit a significant increase in absorbance at wavelengths below 400 nm, corresponding to the ultraviolet (UV) region of the electromagnetic spectrum. The absorption edge, defined as the wavelength at which the absorbance undergoes a sharp rise, is consistently located in the 300 to 400 nm range. This sharp increase reflects the onset of fundamental interband electronic transitions from the valence band to the conduction band, a hallmark of wide bandgap

semiconductor materials (Agrawal *et al.*, 2022; Sharif *et al.*, 2019).

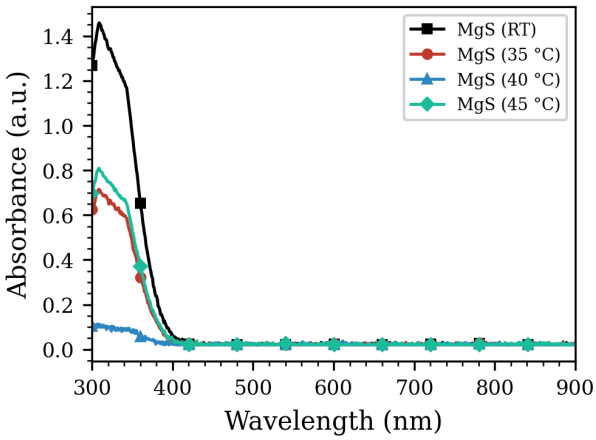

Figure 3: *Absorbance spectra of MgS thin films deposited at room temperature, 35 °C, 40 °C, and 45 °C.*

The room temperature MgS film displays the highest peak absorbance in the UV region, reaching values above 1.5 a.u. at approximately 320 nm. For the heated samples, the maximum absorbance at 300 nm is comparatively lower: MgS 45 °C peaks at approximately 0.85 a.u., MgS 35 °C at 0.75 a.u., and MgS 40 °C exhibits the lowest UV peak at about 0.11 a.u. In the visible spectrum (400 to 700 nm), all films maintain low absorbance values in the range of 0.1 to 0.4 a.u., corresponding to high optical transparency. Small secondary features are visible in the 350 to 450 nm range for the 35 °C and 45 °C samples, which may be attributed to excitonic transitions or to particular structural orientations that develop at those temperatures (Geetha *et al.*, 2017).

3.4 Transmittance

The transmittance spectra of the deposited MgS thin films are shown in Figure 4. A consistent trend is observed across all samples: transmittance is at its lowest in the UV region (below 30%) due to strong fundamental absorption, and increases sharply in the visible and near infrared regions. The MgS 40 °C sample exhibits the highest transparency of all four films, with transmittance values reaching between 90% and 95% across the visible spectrum. This exceptional transparency suggests that 40 °C may represent the optimal deposition temperature for producing films with the fewest structural defects and the best crystallinity for window layer applications (Bradford, 2003; Muthuraj, 2021).

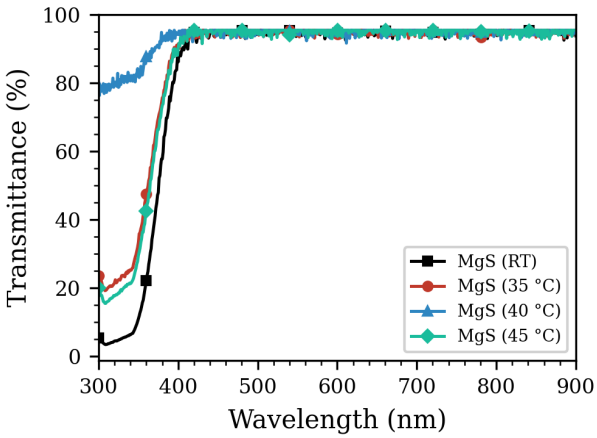

Figure 4: *Transmittance spectra of MgS thin films deposited at room temperature, 35 °C, 40 °C, and 45 °C.*

The MgS 45 °C sample shows transmittance peaking at approximately 65 to 70%, slightly lower than the 40 °C film but still within a range suitable for optoelectronic applications. The room temperature and 35 °C films display similar peak transmittance values around 70 to 75%. The steeper absorption edge observed for the 40 °C and 45 °C films is indicative of improved film quality, as a sharper transition between the opaque UV region and the transparent visible region reflects more homogeneous crystallite sizes and fewer band tail states arising from disorder (Akpu *et al.*, 2023a; Ikhioya and Nkele, 2024).

3.5 Reflectance

The reflectance spectra of the MgS thin films are presented in Figure 5. All samples exhibit a sharp increase in reflectance at shorter wavelengths near the UV region, followed by a peak in the visible range and a general decline towards the near infrared. The MgS 35 °C sample maintains the highest overall reflectance in the visible region, sustaining a level around 20% across a broad spectral window (400 to 700 nm). The MgS 40 °C film shows the lowest reflectance, dropping to a baseline between 4% and 6% across much of the visible spectrum, consistent with its exceptionally high transmittance.

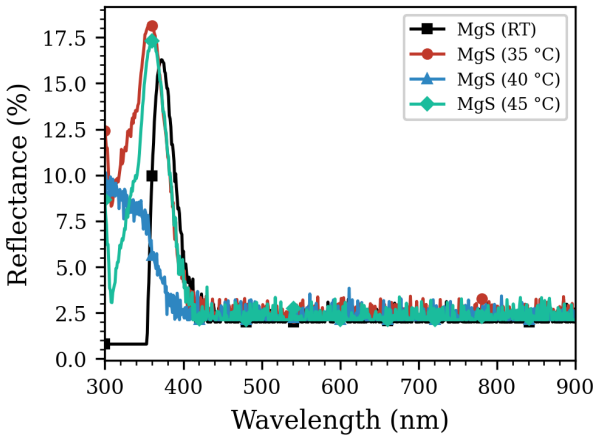

Figure 5: *Reflectance spectra of MgS thin films deposited at room temperature, 35 °C, 40 °C, and 45 °C.*

The low reflectance of the 40 °C sample is a desirable property for anti reflective coatings and solar window layers, where minimising the fraction of light reflected away from the active region is paramount. The variations in reflectance across the temperature series suggest that the 40 °C deposition condition produces a smoother surface morphology or a more favourable refractive index profile compared to the other temperatures (Ijeh *et al.*, 2024; Courage, 2024).

3.6 Optical Band Gap

The optical band gap energies of the MgS thin films were determined from Tauc plots of $(\alpha h\nu)^2$ versus photon energy, assuming a direct allowed transition. The resulting Tauc plots are presented in Figure 6, and the extracted band gap values are summarised alongside a bar chart in Figure 7. A clear monotonic increase in band gap energy with deposition temperature is observed: the room temperature film exhibits a band gap of 1.50 eV, which increases to 2.00 eV at 35 °C, 2.07 eV at 40 °C, and 2.38 eV at 45 °C.

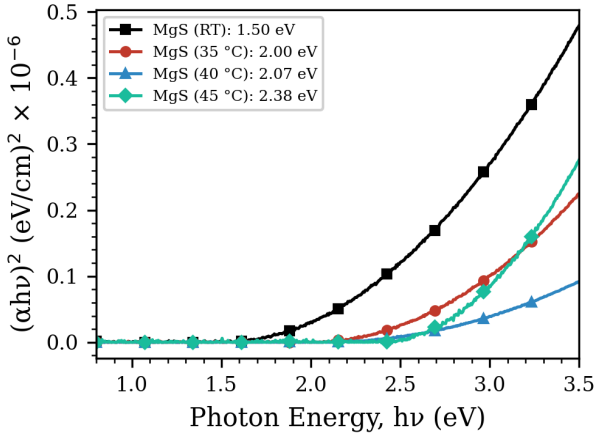

Figure 6: *Tauc plots of $(\alpha h\nu)^2$ versus photon energy for MgS thin films deposited at varying temperatures.*

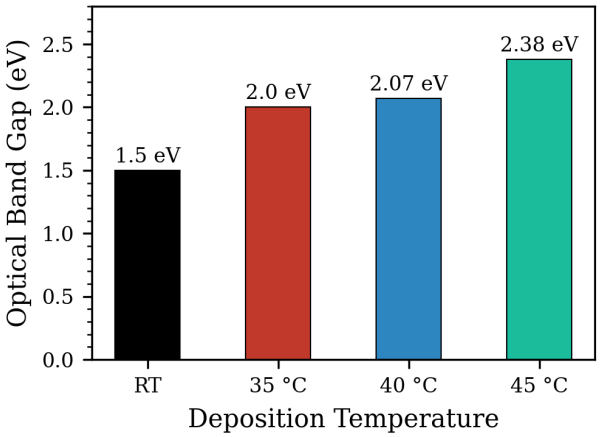

Figure 7: *Variation of optical band gap with deposition temperature for MgS thin films.*

The total shift of 0.88 eV across the temperature range represents a significant blue shift in the optical absorption edge. In thin film semiconductors, a blue shift in the band gap is frequently associated with a decrease in grain size (quantum confinement effects) or with improvements in the stoichiometric ratio and crystalline ordering of the film at elevated synthesis temperatures (Drief *et al.*, 2004; Sharif *et al.*, 2019). The transition from 1.50 eV, which lies near the border of the near infrared and visible regions, to 2.38 eV, which falls in the green to blue portion of the visible spectrum, substantially alters the range of applications for which the material is suited.

Films deposited at higher temperatures are better suited for UV photodetectors and window layers in photovoltaic cells because they remain transparent to a wider range of visible light. The band gap value of 2.38 eV obtained at 45 °C approaches the bulk MgS value of 2.42 eV reported by Agrawal *et al.* (2022), indicating that the higher deposition temperature promotes the formation of a film whose electronic structure closely approximates that of the bulk crystal. These results demonstrate that deposition temperature serves as a critical and readily adjustable tuning parameter for the optical properties of electrochemically deposited MgS thin films (Samuel *et al.*, 2023a; Ikhioya *et al.*, 2023a).

4. Conclusion

Nanocrystalline magnesium sulfide (MgS) thin films were successfully synthesised via the electrochemical deposition technique at four distinct precursor temperatures ranging from room temperature to 45 °C. X ray diffraction analysis confirmed the polycrystalline nature of all films, with four diffraction peaks indexed to the (011), (111), (200), and (211) planes. The preferred orientation along the (111) plane was preserved across all deposition temperatures, and the peak intensities increased

with temperature, indicating enhanced crystallinity.

Electrical measurements revealed a direct proportionality between resistivity and both temperature and film thickness, with the very low conductivity values confirming the wide bandgap semiconducting or near insulating character of the films. Optical characterisation demonstrated high transparency in the visible spectrum for all samples, with the MgS 40 °C film achieving transmittance values exceeding 90%. The optical band gap exhibited a significant blue shift from 1.50 eV at room temperature to 2.38 eV at 45 °C, demonstrating that the deposition temperature is an effective parameter for tuning the electronic structure of MgS thin films.

These findings establish that electrochemically deposited MgS thin films prepared at elevated temperatures are promising candidates for UV photodetectors and window layers in photovoltaic architectures. The films deposited at 40 °C, which exhibit the highest optical transparency and lowest reflectance, are particularly well suited for transparent conducting electrode applications. Future work should examine the surface morphology using scanning electron microscopy and explore the influence of dopant incorporation on the electronic and optical properties of these nanocrystalline MgS films.

Acknowledgments

The authors gratefully acknowledge the Department of Physics, Delta State University, Abraka, and the Department of Physics, Federal University Lokoja, for providing access to laboratory facilities and characterisation equipment.

References

[1] Agrawal, N.K., Gangal, D., Agarwal, R. and Jhakar, N. (2022). Thermal annealing of magnesium sulphide (MgS) thin films: Surface interface studies for energy applications. *AIP Conference Proceedings*, 2265, 26–30. https://doi.org/10.1063/5.0016853

[2] Akpu, N.I., Sylvanus, C.A. and Nwaokorongwu, E.C. (2023a). Modulation of the physical properties of spray deposited cobalt selenide nanofilm via yttrium doping for photovoltaic purposes. *Journal of Science and Technology*, 14(11), 1230–1244.

[3] Akpu, N. (2023b). Impact of temperature difference on the features of spray deposited yttrium doped cobalt selenide (YCoSe) thin films for photovoltaic application. *Advances in Scientific Research*, 2, 143. https://doi.org/10.46481/asr.2023.2.3.143

[4] Ali, A., Afzal, S., Khaleeq, T., Shah, H., Usman, M. and Imosobomeh, L. (2023). Synthesis and characterization of chitosan silver nanocomposite using chemical reduction method and their antibacterial properties. *Journal of Nanomaterials and Nanoengineering*, 2(1), 117–122.

[5] Bradford, C. (2003). Growth and characterization of MgS/CdSe self assembled quantum dots. *Journal of Crystal Growth*, 251(1–4), 581–585. https://doi.org/10.1016/S0022-0248(02)02309-6

[6] Courage, U.I. (2024). Investigating the Linum usitatissimum mucilage synergistic amalgamation of metal oxide electrodes for super capacitive applications. *Journal of the Indian Chemical Society*, 101(12), 101477. https://doi.org/10.1016/j.jics.2024.101477

[7] Drief, F., Tadjer, A., Mesri, D. and Aourag, H. (2004). First principles study of structural, electronic, elastic and optical properties of MgS, MgSe and MgTe. *Catalysis Today*, 89(3), 343–355. https://doi.org/10.1016/j.cattod.2003.12.013

[8] Geetha, G., Murugasen, P. and Sagadevan, S. (2017). Synthesis and characterization of manganese sulphide thin films by chemical bath deposition method. *Acta Physica Polonica A*, 132(4), 1221–1226. https://doi.org/10.12693/APhysPolA.132.1221

[9] Ijeh, F.I., Ikhioya, I.L. and Ezema, F.I. (2024). Synthesis and characterization of copper doped TiO_2 via electrodeposition method for photovoltaic applications. *FUPRE Journal of Scientific and Industrial Research*, 8(4), 339–351.

[10] Ikhioya, I.L. and Nkele, A.C. (2024). Green synthesis and characterization of aluminum oxide nanoparticle using neem leaf extract (Azadirachta indica). *Hybrid Advances*, 5, 100141. https://doi.org/10.1016/j.hybadv.2024.100141

[11] Ikhioya, I.L., Aisida, S.O., Ahmad, I. and Ezema, F.I. (2023a). The effect of molybdenum dopant on rare earth metal chalcogenide material. *Chemical Physics Impact*, 7, 100269. https://doi.org/10.1016/j.chphi.2023.100269

[12] Ikhioya, I.L. and Nkele, A.C. (2023a). A novel synthesis of hydrothermally prepared yttrium selenide and erbium selenide nanomaterials doped with magnesium. *Results in Optics*, 13, 100555. https://doi.org/10.1016/j.rio.2023.100555

[13] Ikhioya, I.L. and Nkele, A.C. (2023b). Properties of electrochemically deposited NiTe films doped with molybdenum at varying temperatures. *Results in Optics*, 12, 100494. https://doi.org/10.1016/j.rio.2023.100494

[14] Ikhioya, I.L. and Nkele, A.C. (2023c). Properties of electrochemically deposited NiTe films prepared at varying dopant concentrations of molybdenum. *Journal of Materials Science: Materials in Electronics*, 34(21). https://doi.org/10.1007/s10854-023-11018-0

[15] Ikhioya, I.L., Nkele, A.C. and Ochai-Ejeh, F.U. (2023). Green synthesis of copper oxide nanoparticle using neem leaf extract (Azadirachta indica) for energy storage applications. *International Journal of Green Energy*, 00(00), 1–7. https://doi.org/10.1080/14328917.2023.2252677

[16] Muthuraj, D. (2021). Magnesium polysulfide catholyte (MgSx): Synthesis, electrochemical and computational study for magnesium sulfur battery application. *Journal of Power Sources*, 486, 229326. https://doi.org/10.1016/j.jpowsour.2020.229326

[17] Okechukwu, E.O., Ikhioya, I.L. and Ekpunobi, A.J. (2024). Effect of precursor pH on the electrochemically synthesised barium titanium sulphide (BaTiS) material for photovoltaic application. *International Journal of Green Energy*, 00(00), 1–10. https://doi.org/10.1080/14328917.2024.2376377

[18] Onyebuchi, A.C. (2026). Microwave synthesis and characterization of calcium copper titanate oxide and composites for supercapacitor applications. *Next Materials*, 10, 101585. https://doi.org/10.1016/j.nxmate.2026.101585

[19] Saba, S., Alsharari, A.M., Aldaleeli, N.Y., Aljohani, M.M. and Hamdalla, T.A. (2025). Structural, electrochemical, and supercapacitor characterization of double metal oxides doped within ZIF 8 composites. *Processes*, 13(3), 859. https://doi.org/10.3390/pr13030859

[20] Samuel, S.O., Frank, M.L.E., Ogherohwo, E.P., Ekpekpo, A., Zhimwang, J.T. and Ikhioya, I.L. (2023a). Influence of deposition voltage on strontium sulphide doped silver for optoelectronic application. *East European Journal of Physics*, 2023(1), 189–196. https://doi.org/10.26565/2312-4334-2023-1-25

[21] Samuel, S.O. (2023b). The influence of precursor temperature on strontium sulphide doped silver for optoelectronic application. *Journal of the Indian Chemical Society*, 100(5), 100992. https://doi.org/10.1016/j.jics.2023.100992

[22] Sarwar, S.G., Ikhioya, I.L., Afzal, S. and Ahmad, I. (2023). Supercapacitance performance evaluation of MXene/Graphene/NiO composite electrode via in situ precipitation technique. *Hybrid Advances*, 4, 100105. https://doi.org/10.1016/j.hybadv.2023.100105

[23] Sharif, S., Ahmad, K.S., Akhtar, M.S., Mehmood, R.F., Alamgir, M.K. and Malik, M.A. (2019). In situ synthesis and deposition of un doped and doped magnesium sulfide thin films by green technique. *Optik*, 182, 739–744. https://doi.org/10.1016/j.ijleo.2018.12.108